Examining the number of required stationary orientations for efficient accelerometer calibration

Peter Sarcevic
Technical Department
University of Szeged
Szeged, Hungary
sarcevic@mk.u-szeged.hu

Szilveszter Pletl, Zoltan Kincses
Department of Technical Informatics
University of Szeged
Szeged, Hungary
pletl@inf.u-szeged.hu, kincsesz@inf.u-szeged.hu

***Abstract*— Nowadays, accelerometers are used in a large variety of applications. These sensors suffer from various types of deterministic and stochastic errors. Deterministic errors are caused by manufacturing defects, and include bias, scale factor, and misalignment errors. These errors can be compensated by calibrating the sensors, during which calibration parameters are computed. Previously, the authors proposed an evolutionary algorithm-based solution for efficient accelerometer calibration, which utilizes stationary measurements from several different orientations. In this paper, the number of required orientations is investigated which is required to achieve still precise measurements. The algorithm is tested using real measurement data, collected from multiple sensors. The obtained results show, that six basic orientations are required for efficient calibration of the sensors, but slight improvements can be achieved if more orientations are applied.**

Keywords*— *accelerometer; sensor calibration; evolutionary algorithm

I. INTRODUCTION

An accelerometer detects specific force, which is proportionate to the acceleration of the sensor in its axis of sensitivity. With the developments in Micro-Electro-Mechanical Systems (MEMS), the availability of small, lower-cost, medium-performance inertial sensors have opened new possibilities for their use. These sensors can be used in a large variety of applications, like navigation [1], pattern recognition [2], vibration analysis [3-4], vehicle detection and classification [5-6], etc.

Accelerometers suffer from various types of errors that can be classified as deterministic or systematic errors and random or stochastic errors [7]. The calibration is a process of comparing the sensor's output with the known reference information to estimate these error coefficients, which form an exact relationship between observed readings and expected outputs. Deterministic errors occur due to manufacturing defects, and can be calibrated using the fact that the vector magnitude should be 1 g when the sensor is not in movement. To obtain the linear position, accelerometer measurements need to integrated twice. Because of the integration process, even very small errors at the output accumulate very rapidly and the position error becomes considerably large.

Calibration can be done with and without additional equipment. High-precision equipment can be used in laboratory environment to generate known references which can be compared with the sensors outputs. Due to the growing usage of accelerometers, and unavailability and high cost of calibration equipment, in recent years, intensive research was done to develop calibration methods which do not require additional equipment.

The computation of the calibration parameters can be done online and offline. In case of online calibration, the parameters are computed in real-time on the measurement device, while in offline algorithms previously collected measurements are used.

In the literature, various algorithms exist for the calibration accelerometer sensors. The known algorithms mainly apply a six-position test, where during the measurements the three axes of the sensors are aligned to be nearly +1 g and -1 g [7].

In [8], a non-iterative algorithm was proposed, which focuses on minimal execution time and low memory consumption. The method works in two steps: first, the center of the ellipsoid is estimated, and then the scale factors are computed. The aim of both steps is to form and solve a system of linear equations with the same number of equations and unknown variables using the least-square method.

Kalman Filter-based approaches are very popular in the field of sensor calibration [9-11].

Various optimization techniques were also tested in reported works. In [12], a geometric ellipsoid parameter estimation technique was applied, that uses the Levenberg-Marquardt algorithm (LMA) to perform nonlinear optimization. An offline calibration method using the Maximum Likelihood Estimation (MLE) was tested in [13]. Gao et al. proposed a method based on the Artificial Fish Swarm Algorithm (AFSA) for the identification of error coefficients [14], whereas Particle Swarm Optimization (PSO) was utilized in [1].

Previously, an evolutionary algorithm-based offline approach was proposed in [15], which applied stationary measurements from 80 different orientations for efficient accelerometer calibration. The solution does not require any

additional high-precision equipment. In this study, the number of required orientations is investigated, which is required for efficient calibration of the sensors.

II. SENSOR MODELS

The deterministic errors that affect the system performance are most commonly represented by bias, scale factor, and nonorthogonality, whereas the random errors are modeled stochastically. Deterministic errors can be calculated during sensor calibration and they can be compensated later during real-time work. Random errors occur due to random fluctuations in the system response and cannot be predicted or compensated. In this research, all three deterministic error types were investigated.

A. Standard model

Bias in the accelerometer output will cause a shift in the measured acceleration vector from its real direction.

$$\boldsymbol{b} = \begin{bmatrix} b_x \\ b_y \\ b_z \end{bmatrix}, \tag{1}$$

where b_x, b_y, and b_z in the $\boldsymbol{b}$ bias vector are the bias values on each axis.

Scale factors determine the sensor's sensitivity to the intended acceleration at each axis. The matrix consisting the scale factors can be represented as:

$$\boldsymbol{S} = \begin{bmatrix} S_x & 0 & 0 \\ 0 & S_y & 0 \\ 0 & 0 & S_z \end{bmatrix}, \tag{2}$$

where S_x, S_y, and S_z are the scale factors for each axis.

Nonorthogonality between axes is the inaccuracy resulting from the imperfection in sensor mounting during its manufacturing. Misalignment errors are, however, introduced due to nonalignment of sensor's sensitive axis and the mounting platform.

$$\boldsymbol{M} = \begin{bmatrix} 1 & m_{xy} & m_{xz} \\ m_{yx} & 1 & m_{yz} \\ m_{zx} & m_{zy} & 1 \end{bmatrix}, \tag{3}$$

where m_{xy}, m_{xz}, m_{yx}, m_{yz}, m_{zx}, and m_{zy} in the $\boldsymbol{M}$ matrix are the misalignment error coefficients.

The relation between the measured and the real values can be given as:

$$\begin{bmatrix} r_x \\ r_y \\ r_z \end{bmatrix} = \begin{bmatrix} 1 & m_{xy} & m_{xz} \\ m_{yx} & 1 & m_{yz} \\ m_{zx} & m_{zy} & 1 \end{bmatrix} \begin{bmatrix} S_x & 0 & 0 \\ 0 & S_y & 0 \\ 0 & 0 & S_z \end{bmatrix} \begin{bmatrix} o_x \\ o_y \\ o_z \end{bmatrix} + \begin{bmatrix} b_x \\ b_y \\ b_z \end{bmatrix} + \begin{bmatrix} \eta_x \\ \eta_y \\ \eta_z \end{bmatrix}, \tag{4}$$

where o_x, o_y, and o_z are the measured sensor outputs, while r_x, r_y, and r_z are the real acceleration values on each axis. The terms η_x, η_y, and η_z assign the noise values that are generally assumed to be white Gaussian.

Combining the $\boldsymbol{M}$ and $\boldsymbol{S}$ matrices into one matrix, a calibration model utilizing 12 parameters can be given as:

$$\begin{bmatrix} r_x \\ r_y \\ r_z \end{bmatrix} = \begin{bmatrix} m_{xx} & m_{xy} & m_{xz} \\ m_{yx} & m_{yy} & m_{yz} \\ m_{zx} & m_{zy} & m_{zz} \end{bmatrix} \begin{bmatrix} o_x \\ o_y \\ o_z \end{bmatrix} + \begin{bmatrix} b_x \\ b_y \\ b_z \end{bmatrix}. \tag{5}$$

B. Simplified model

A simplified relation, which applies 9 parameters, can be given using the model seen in Fig. 1. The misalignment error matrix can be given as:

$$M = \begin{bmatrix} 1 & 0 & 0 \\ -\sin(\alpha_{zy}) & \cos(\alpha_{zy}) & 0 \\ -\sin(\alpha_{yz}) & -\sin(\alpha_{xz})\cos(\alpha_{yz}) & \cos(\alpha_{xz})\cos(\alpha_{yz}) \end{bmatrix}, \tag{6}$$

where α_{zy}, α_{xz}, and α_{yz} are the misalignment angles.

III. DATA ACQUISITION

Do to their small size and easy programming, wireless sensor motes were used for data acquisition, which are a widely-used platform for the implementation of different Wireless Sensor Networks (WSNs) [16-18].

IRIS motes were utilized, which are built-up of from an Atmel ATmega 1281L 8-bit microcontroller and an RF231 IEEE 802.15.4 compatible radio transceiver. The highest data throughput of the radio transceiver is 250 kbps, and it has outdoor range over 300 m. To perform the measurements, 9 degree of freedom (9DOF) sensor boards were connected to the IRIS motes using the MDA100 prototyping board. The connected 9DOF sensor board is made up of an ADXL345 tri-axial MEMS accelerometer, an ITG3200 tri-axial MEMS gyroscope, and an HMC5883L tri-axial magnetoresistive technology-based magnetometer. The ADXL345 is a low power accelerometer (the current draw is 40 µA in measurement mode, and 0.1 µA in sleep mode), which can measure up to ±16 g in 13-bit resolution with a highest sampling rate of 3.2 kHz. The IRIS mote and the connected sensor board can be seen on Fig. 2.

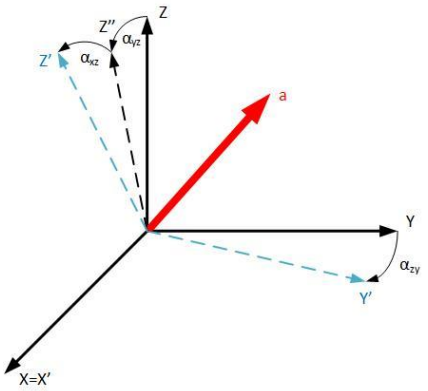

Fig. 1. Simplified sensor model

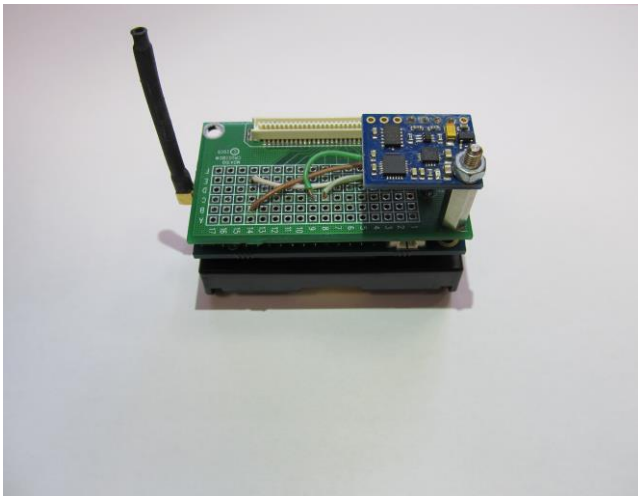

Fig. 2. The sensor board connected to the IRIS mote

In the field of WSNs, TinyOS is the most widely used, event-driven operating system. An application was developed to configure the sensors and cyclically read the measurement data via the I2C interface, and to send the data to a so-called BaseStation mote via wireless communication. The BaseStation mote forwards the received data to a PC, where an application stores them to a database. The collected measurement data can be later visualized [19], and used in offline algorithms.

Data acquisition was done using three different sensor boards, with an applied sampling rate of 125 Hz. Measurement data were collected in 80 different orientations, and 200 measurements were saved for every setup. These orientations consist 10 basic orientations, around which measurements were done in 8 orientations. The basic orientations were chosen where the acceleration values should be nearly +1 g and -1 g in the *X*, *Y*, and *Z* axes, while in the remaining 2 basic orientations none of the three sensor axes should be 0.

IV. Calibration algorithm

The measurement values are first transformed into g-s, since the algorithm later uses the fact that the magnitude should be 1 g when the sensor is not in movement.

The calibration parameters in the models are double type values, and they form the phenotype for the evolutionary algorithm. To accelerate the optimization, a priori knowledge is added to the method in the form of parameter ranges. In the fitness function, the output vector is computed for each measurement vector using the current calibration parameters. The magnitudes are then calculated for all measurements using (7), and the Mean Squared Error (MSE), as given in (8), is calculated based on the differences between the computed magnitudes and the expected 1 g acceleration. The goal of the optimization is to minimize the MSE value.

$$mag = \sqrt{r_x^2 + r_y^2 + r_z^2} \tag{7}$$

$$mse = \frac{1}{N}\sum_{i=1}^{N}(1 - mag_i)^2, \tag{8}$$

where N is the number of measurements, and mag_i is the magnitude of the ith measurement.

V. Experimental results

Using the measurement data collected in 80 orientations, based on the selection of which to be utilized as training and which as validation data, altogether 7 combinations were defined. The used orientations in the training data in the seven combinations are the next:

1. $X \approx +1$ g, $Y \approx +1$ g, $Z \approx +1$ g; only one orientation for all three basic orientations,
2. $X \approx +1$ g, $Y \approx +1$ g, $Z \approx +1$ g; all 8 orientations for all three basic orientations,
3. $X \approx -1$ g, $Y \approx -1$ g, $Z \approx -1$ g; only one orientation for all three basic orientations,
4. $X \approx -1$ g, $Y \approx -1$ g, $Z \approx -1$ g; all 8 orientations for all three basic orientations,
5. $X \approx +1$ g, $Y \approx +1$ g, $Z \approx +1$ g, $X \approx -1$ g, $Y \approx -1$ g, $Z \approx -1$ g; only one orientation for all three basic orientations
6. $X \approx +1$ g, $Y \approx +1$ g, $Z \approx +1$ g, $X \approx -1$ g, $Y \approx -1$ g, $Z \approx -1$ g; all 8 orientations for all three basic orientations,
7. All 80 orientations.

The validation datasets were constructed utilizing all orientations which were not the part of the training data. Using the previously described combinations, it can be examined that how much can the orientations in the basic orientations improve the results.

The optimization of the calibration parameters was performed for all seven combinations, and for all three sensors, using the simplified sensor model.

Table 1 shows the MSE values and the highest differences from the 1 g magnitude on training and validation measurements for all seven combinations. Since in the last combination all orientations were applied in the training datasets, no data were used as validation measurements, thus, no MSE values and highest difference values are available. The results show, that measurements in six basic orientations are necessary for efficient calibration of the sensors. The MSE values and highest differences show high errors when combinations 1-4 were applied. The obtained MSE values on training data in combinations 5 and 6 are nearly equal with the results achieved with utilizing all orientations during the optimization (combination 7). The MSE values on validation measurements are slightly higher than on training data, which shows that still slight improvements can be achieved if more basic orientations are utilized. The highest differences to the 1 g magnitude level are nearly equal in case of training and validation measurements, and are around 25 mg for all three sensors, which is the peak-to-peak random noise level.

VI. Conclusion

In this paper, the number of required orientations were investigated for effective accelerometer calibration. A previously proposed, evolutionary algorithm-based method was applied for the optimization of the calibration parameters utilizing a simplified (9 parameter) model.

TABLE I. ACHIEVED MSE VALUES AND HIGHEST DIFFERENCES ON TRAINING AND VALIDATION DATA USING DIFFERENT ORIENTATION COMBINATIONS

		Defined orientation combinations						
		1	*2*	*3*	*4*	*5*	*6*	*7*
MSE on training data	***Sensor 1***	0.000027	0.000023	0.000023	0.000027	0.000024	0.000025	0.000025
	Sensor 2	0.000035	0.000028	0.000026	0.000025	0.000029	0.000028	0.000034
	Sensor 3	0.000024	0.000024	0.000030	0.000026	0.000029	0.000028	0.000032
MSE on validation data	***Sensor 1***	0.010247	0.003710	0.007419	0.015416	0.000025	0.000027	-
	Sensor 2	0.032212	0.002336	0.004026	0.040625	0.000035	0.000046	-
	Sensor 3	0.010865	0.003739	0.005259	0.070210	0.000035	0.000044	-
Highest difference on training data	***Sensor 1***	0.01810	0.01922	0.01850	0.02860	0.01880	0.02630	0.02630
	Sensor 2	0.02163	0.02370	0.01904	0.02070	0.02310	0.02480	0.03033
	Sensor 3	0.01644	0.01980	0.02544	0.01990	0.02597	0.0257	0.02562
Highest difference on validation data	***Sensor 1***	0.23650	0.11788	0.15663	0.20930	0.02680	0.01890	-
	Sensor 2	0.40630	0.11918	0.12931	0.34709	0.03066	0.03068	-
	Sensor 3	0.23119	0.15852	0.1974	0.36144	0.02672	0.02644	-

The results show, that measurements in six basic orientations are at least required for efficient accelerometer calibration. The obtained MSE values on training data when the six basic orientations are applied are nearly equal with the results achieved with utilizing all orientations during the optimization. The MSE values on validation measurements are slightly higher than on training data when only six orientations are utilized, what shows that still slight improvements can be achieved if more basic orientations are used. The highest differences to the 1 g magnitude level are around 25 mg for all three sensors, which is the peak-to-peak random noise level.

REFERENCES

[1] Q. Cai, N. Song, G. Yang, and Y. Liu, "Accelerometer calibration with nonlinear scale factor based on multi-position observation," Meas. Sci. Technol., vol. 24, 105002, August 2013.

[2] P. Sarcevic, L. Schaffer, Z. Kincses, and S. Pletl, "Hierarchical-distributed approach to movement classification using wrist-mounted wireless inertial and magnetic sensors," Infocommunications J., vol. 7, pp. 33-41, September 2015.

[3] L. Cveticanin, I. Biro, J. Sarosi, and M. Zukovic, "Axial vibration of an artificial muscle," International Conference on Bioinformatics and Bioengineering (BIBE), pp. 1-5, 2015.

[4] L. Cveticanin, M. Zukovic, G. Mester, I. Biro, and J. Sarosi, "Oscillators with symmetric and asymmetric quadratic nonlinearity," Acta Mech., vol. 227, pp. 1727-1742, June 2016.

[5] J. Smidla and G. Simon, "Accelerometer-based event detector for low-power applications," Sens., vol. 13, pp. 13978-13997, October 2013.

[6] W. Ma, et al., "A wireless accelerometer-based automatic vehicle classification prototype system," IEEE Trans. Intell. Transp. Syst., vol. 15, pp. 104-111, February 2014.

[7] S. Poddar, V. Kumar, and A. Kumar, "A comprehensive overview of inertial sensor calibration techniques," J. Dyn. Sys., Meas., Control, vol. 139, 011006, January 2017.

[8] M. Gietzelt, K.-H. Wolf, M. Marschollek, and R. Haux, "Performance comparison of accelerometer calibration algorithms based on 3D-ellipsoid fitting methods," Comput. Methods Programs Biomed., vol. 111, pp. 62-71, July 2013.

[9] D. Nemec, A. Janota, M. Hrubos, and V. Simak, "Intelligent real-time MEMS sensor fusion and calibration," IEEE Sens. J., vol. 16, pp. 7150-7160, October 2016.

[10] M. Glueck, D. Oshinubi, P. Schopp, and Y. Manoli, "Real-time autocalibration of MEMS accelerometers," IEEE Trans. Instrum. Meas., vol. 63, pp. 96-105, January 2014.

[11] T. Bevars, J. Podobnik, M. Munih, "Three-axial accelerometer calibration using Kalman filter covariance matrix for online estimation of optimal sensor orientation," IEEE. Trans. Instrum. Meas., vol. 61, pp. 2501-2511, September 2012.

[12] G. Secer and B. Barshan, "Improvements in deterministic error modeling and calibration of inertial sensors and magnetometers," Sens. Actuators A: Phys, vol. 247, pp. 522-538, August 2016.

[13] X. Lu, Z. Liu, and J. He, "Maximum likelihood approach for low-cost MEMS triaxial accelerometer calibration," International Conference on Intelligent Human-Machine Systems and Cybernetics (IHMSC), pp. 179-182, 2016.

[14] Y. Gao, L. Guan, and T. Wang, "Triaxial accelerometer error coefficients identification with a novel artificial fish swarm algorithm," J. Sens., vol. 2015, 509143, May 2015.

[15] P. Sarcevic, S. Pletl, and Z. Kincses, "Evolutionary algorithm based 9DOF sensor board calibration," International Symposium on Intelligent Systems and Informatics (SISY), pp. 187-192, 2014.

[16] L. Gogolak, I. Furstner, and S. Pletl, "Wireless sensor network based localization in industrial environments," Analecta Tech. Szegedinensia, vol. 8, pp. 91-96, July 2014.

[17] L. Gogolak, S. Pletl, and D. Kukolj, "Neural Network-based Indoor Localization in WSN Environments," Acta Polytech. Hungarica, vol. 10, pp. 221-235, 2013.

[18] J. Simon and G. Martinovic, "Navigation of Mobile Robots Using WSN's RSSI Parameter and Potential Field Method," Acta Polytech. Hungarica, vol. 10, pp. 107-118, 2013.

[19] J. Sarosi, Measurement and Data Acquisition. University of Szeged, Faculty of Engineering, Szeged, Hungary: 2014.